Proc. Natl. Acad. Sci. USA
Vol. 93, pp. 6998–7002, July 1996
Biochemistry

Kinetics of photo-induced electron transfer from high-potential iron–sulfur protein to the photosynthetic reaction center of the purple phototroph *Rhodoferax fermentans*

(bacterial photosynthesis)

A. HOCHKOEPPLER*, D. ZANNONI*, S. CIURLI†‡, T. E. MEYER§, M. A. CUSANOVICH§, AND G. TOLLIN§

*Department of Biology, University of Bologna, I-40126 Bologna, Italy; †Institute of Agricultural Chemistry, University of Bologna, I-40127 Bologna, Italy; and §Department of Biochemistry, University of Arizona, Tucson, AZ 85721

Communicated by Richard H. Holm, Harvard University, Cambridge, MA, March 13, 1996 (received for review December 4, 1995)

ABSTRACT **The kinetics of photo-induced electron transfer from high-potential iron–sulfur protein (HiPIP) to the photosynthetic reaction center (RC) of the purple phototroph *Rhodoferax fermentans* were studied. The rapid photooxidation of heme c-556 belonging to RC is followed, in the presence of HiPIP, by a slower reduction having a second-order rate constant of $4.8 \times 10^7\ M^{-1}\cdot s^{-1}$. The limiting value of k_{obs} at high HiPIP concentration is $95\ s^{-1}$. The amplitude of this slow process decreases with increasing HiPIP concentration. The amplitude of a faster phase, observed at 556 and 425 nm and involving heme c-556 reduction, increases proportionately. The rate constant of this fast phase, determined at 425 and 556 nm, is $\approx 3 \times 10^5\ s^{-1}$. This value is not dependent on HiPIP concentration, indicating that it is related to a first-order process. These observations are interpreted as evidence for the formation of a HiPIP–RC complex prior to the excitation flash, having a dissociation constant of $\approx 2.5\ \mu M$. The fast phase is absent at high ionic strength, indicating that the complex involves mainly electrostatic interactions. The ionic strength dependence of k_{obs} for the slow phase yields a second-order rate constant at infinite ionic strength of $5.4 \times 10^6\ M^{-1}\cdot s^{-1}$ and an electrostatic interaction energy of −2.1 kcal/mol (1 cal = 4.184 J). We conclude that *Rhodoferax fermentans* HiPIP is a very effective electron donor to the photosynthetic RC.**

Anoxygenic phototrophic bacteria contain two membrane-bound components that are essential for energy production, the photosynthetic reaction center (RC) and the cytochrome bc_1 complex. Two types of RC have been structurally characterized: the RC from *Rhodobacter sphaeroides* is made of three subunits (1, 2), while, in addition to these, RC from *Rhodopseudomonas viridis* contains a fourth tetraheme cytochrome *c* subunit (2, 3). In *Rps. viridis* the four heme groups have α bands at 559, 552, 556, and 554 nm, and reduction potentials of +380 mV, +20 mV, +310 mV, and −60 mV, respectively (4). The four hemes are arranged in an almost linear fashion, (2, 5, 6) and are aligned in the sequence P/c-559/c-552/c-556/c-554, where P indicates the bacteriochlorophyll special pair (4, 7). The highest potential heme (c-559) is oxidized the most rapidly ($t_{1/2} \approx 300$ ns) by the photooxidized P (P^+), followed by a slower oxidation of heme c-556 ($t_{1/2} \approx 2\ \mu s$) (4, 8, 9). The quinol generated by RC photooxidation is utilized by the bc_1 complex to reduce cytochrome c_2 (10), a soluble protein closely related to mitochondrial cytochrome *c* (11, 12). Cytochrome c_2 then reduces the photooxidized RC, closing the photocycle. However, although cytochrome c_2 reacts directly with P^+ in *Rb. sphaeroides* (13–21), in *Rps. viridis*, it reacts with the tetraheme subunit (22–24). Only about half of the purple bacterial species described so far contain cytochrome c_2 (25), and it is not known how the remaining species carry out electron transfer between the bc_1 and RC complexes.

The RC from the purple nonsulfur bacterium *Rhodoferax fermentans* (26) is similar to that of *Rps. viridis* in that it contains a bound tetraheme subunit (27). The four hemes have reduction potentials of +354 mV (c-556), +294 mV (c-560), +79 mV (c-551), and 0 mV (27). *Rf. fermentans* contains a bc_1 complex (28) but does not appear to express a cytochrome c_2 under photosynthetic conditions; instead, a high-potential iron–sulfur protein (HiPIP) is the most abundant high-reduction potential electron carrier ($E_{m,7} = +351$ mV) in the soluble fraction (29). HiPIPs are abundant in most species of purple phototrophic bacteria that lack cytochrome c_2 (25). They have been extensively investigated as electron-transfer models (24, 30–33), and their structural and spectroscopic properties are well characterized (34). Although they have the right reduction potential (+90 to +450 mV) to couple bc_1 and RC complexes (32), suggesting a role in cyclic photosynthetic electron transfer, their physiological function is still a matter for discussion. Earlier reports on the interaction between HiPIP and photosynthetic RC from *Chromatium vinosum* (35–37) and recent evidence suggesting that HiPIP is photooxidized by P^+ in a fast (submillisecond) and a slow (millisecond) phase in *Rf. fermentans* (29, 38) support the concept that HiPIPs may play a role in the photocyclic electron transfer of purple bacteria. Evidence for the presence of a submillisecond electron transfer process was also recently reported in *Rubrivivax gelatinosus* (39). Such a fast phase was observed only in whole cells, whereas *in vitro* a slower electron transfer occurs within an electrostatic complex ($K_d = 5.7\ \mu M$) between HiPIP and RC, with a limiting rate constant of $74.4\ s^{-1}$ (39). To our knowledge, no detailed kinetics data for the fast phase have been reported so far.

The goal of the present study is the elucidation of the mechanism, and the determination of the rate constants, of photo-induced reduction of RC by HiPIP, both isolated from *Rf. fermentans*.

MATERIALS AND METHODS

Cell Growth and Lysis. *Rf. fermentans* cells were grown under anaerobic photoheterotrophic conditions as described (26). Cell harvesting, lysis, and membrane fragment isolation were performed as reported (29).

Protein Purification. The membrane suspension was diluted to yield an absorbance at 800 nm equal to 50 in 10 mM Tris·HCl buffer, pH 8, containing 1 mM EDTA, 100 mM NaCl, and concentrations of lauryldimethylamino-*N*-oxide (LDAO)

The publication costs of this article were defrayed in part by page charge payment. This article must therefore be hereby marked "*advertisement*" in accordance with 18 U.S.C. §1734 solely to indicate this fact.

Abbreviations: RC, reaction center; HiPIP, high-potential iron–sulfur protein; LHI and LHII, light harvesting complexes I and II, respectively; LDAO, lauryldimethylamino-*N*-oxide.

‡To whom reprint requests should be addressed.

from 0.1 to 0.5%. Immediately after addition of detergent, the samples were incubated in a rotary shaker (120 rpm) for 1 h at 25°C in the dark. The resulting suspension was centrifuged at 130,000 × *g* (1.5 h) and the supernatant was collected. At LDAO concentrations higher than 0.4%, the light-harvesting complex II (LHII) was always extracted with RC, while in the range 0.2–0.35%, it was possible to obtain LHII-free preparations of RC associated with light-harvesting complex I (LHI). After LDAO solubilization, the RC–LHI complex was immediately diluted with ice-cold 10 mM Tris·HCl (pH 8)/1 mM EDTA (buffer A). The sample was then concentrated with an Amicon YM100 ultrafiltration membrane and then loaded onto a DEAE-cellulose column (2.6 × 20 cm). The unretained pigments were extensively washed out using buffer A containing 0.025% LDAO, and subsequently a linear NaCl gradient (10–50 mM) was used to elute the RC at ≈35 mM NaCl. The fractions containing purified RC were collected and concentrated again in 10 mM Tris·HCl (pH 8) containing 0.015% LDAO. Purity was checked by SDS/PAGE, using 15% polyacrylamide gels. The soluble cell extract was used for the purification of HiPIP as described (29).

HiPIP and RC concentrations were determined using absorption coefficients of 44 $mM^{-1} \cdot cm^{-1}$ at 278 nm and 288 mM^{-1} cm^{-1} at 802 nm for HiPIP (29) and RC (14), respectively. The reduced-minus-oxidized spectrum of RC was obtained using excess sodium ascorbate as reductant and excess potassium hexacyanoferrate(III) as oxidant.

Kinetic Spectrophotometry. Measurement of transient light-induced absorbance changes were performed as described (24, 40). Excitation was at 610 nm. Errors in rate constants are estimated to be ≤10%. Experiments were performed aerobically in 5- or 10-mm cuvettes with 10 mM Tris·HCl (pH 8) containing 0.015% LDAO and 1 mM ascorbate, prepared fresh daily. The light-induced absorbance changes observed at 556 nm were corrected by subtracting the corresponding signals at 540 nm as described (27). The absorbance changes at 425 nm were corrected by subtracting the corresponding signals observed at 435 nm. This wavelength is an isosbestic point of heme c-556, determined by subtracting the photo-induced difference spectrum recorded in the presence of hexacyanoferrate(II)/(III) (each at 250 μM) from the spectrum obtained in the presence of 1 mM sodium ascorbate.

RESULTS AND DISCUSSION

The absorption spectrum of purified RC is shown in Fig. 1*A*. This spectrum shows the sharp absorption bands of LHI (at 875 nm), of RC accessory bacteriochlorophyll and bacteriopheophytin (at 802 and 756 nm, respectively), and of LHI-bound carotenoids (at 506 and 476 nm). The Q_x transition band of bacteriochlorophyll is also visible at 590 nm. The tetraheme subunit of *Rf. fermentans* RC was found to be loosely bound to the RC core subunits, as reported also for other bacterial species (41). In particular, as also observed with *Ru. gelatinosus* RC (42), the tetraheme subunit was detached from the RC core in all attempts to obtain LHI-free RC preparations. The Soret and α bands relative to the heme prosthetic groups of the latter subunit are visible in the reduced-minus-oxidized spectrum shown in Fig. 1*A Inset* (absorption ratio 425 nm/556 nm = 4.4:1). The difference spectra induced by a single-turnover laser flash excitation, recorded in the range 540–570 and 413–435 nm in the absence of HiPIP show the peaks relative to α (Fig. 1*B*) and Soret bands (Fig. 1*C*), taken 10 and 40 ms after the excitation flash. No significant absorbance changes are observed within this time interval. These spectra and their 425-nm/556-nm absorbance ratio, equal to 3.9:1, indicate that c-556, the highest potential heme group of the RC tetraheme subunit (27), is the predominantly reduced heme under our experimental conditions. This observation was confirmed by analyzing the reduced-minus-oxidized spectra of RC, which indicate that heme c-560 ($E_{m,7}$ = +294 mV) is completely reduced by excess sodium ascorbate only in the presence of the redox mediator tetramethyl *p*-phenylenediamine (DAD).

When the time course of the photooxidation was monitored at 425 nm in the absence of HiPIP, using a time resolution of 140 μs, a rapid decrease of absorbance immediately after the flash was observed, indicating heme c-556 oxidation, and no further absorbance changes were detected up to 80 ms (Fig. 2*A*). In the presence of reduced HiPIP at initial substoichiometric concentrations with respect to RC, on the other hand, reduction of heme c-556 was observed (Fig. 2*B*). The amplitude of this reduction slow phase increased with HiPIP concentration (Fig. 2*C*) and then decreased drastically in the presence of excess HiPIP (Fig. 2*D*), suggesting the presence of a faster phase not observable with this time resolution.

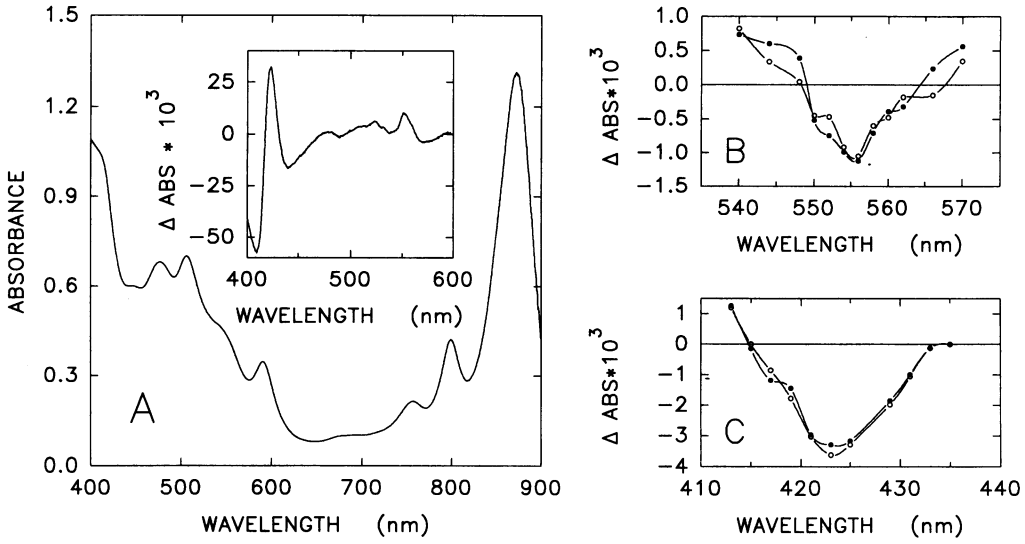

FIG. 1. (*A*) Absolute absorption spectrum of the *Rf. fermentans* RC in 10 mM Tris·HCl, pH 8/0.015% LDAO. (*Inset*) Difference (reduced-minus-oxidized) spectrum in the 400- to 600-nm wavelength interval. (*B*) Difference (photooxidized minus reduced) spectrum of RC (540–570 nm) determined 10 ms (solid circles) and 40 ms (open circles) after the excitation flash. [RC] = 3.3 μM. (*C*) Difference (photooxidized minus reduced) spectrum of RC (413–435 nm) determined 10 ms (solid circles) and 40 ms (open circles) after the excitation flash. [RC] = 2.5 μM.

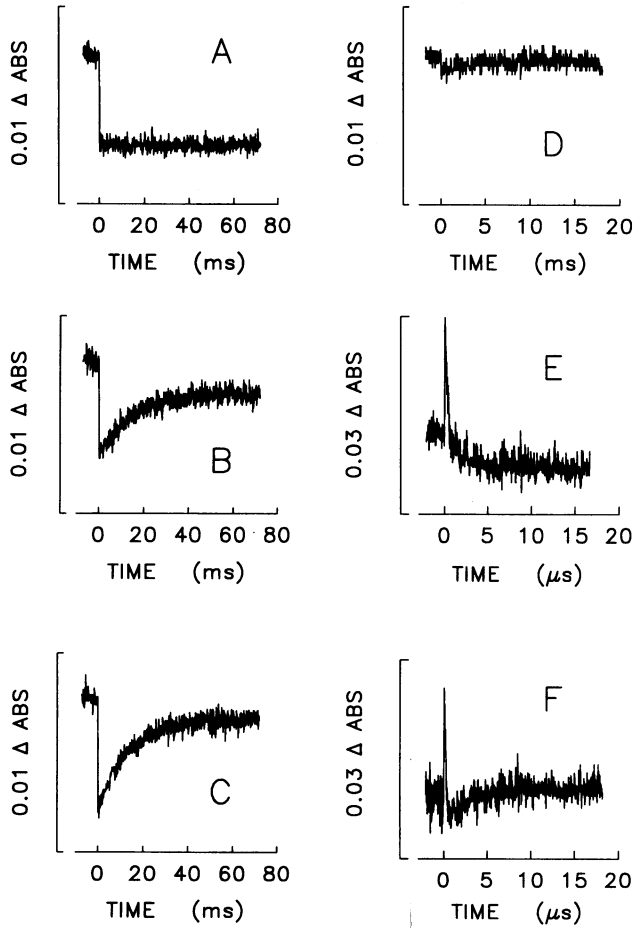

FIG. 2. Light-induced absorbance changes detected at 425 nm using a time resolution of 140 μs (*A–D*) or 35 ns (*E* and *F*) in the absence (*A* and *E*) or in the presence of 3.1 μM (*B*), 5.1 μM (*C*), and 7.7 μM (*D* and *F*) HiPIP. [RC] = 2.5 μM.

By increasing the time resolution to 35 ns, and following the photooxidation at 425 nm in the absence of HiPIP, it was possible to observe an initial very fast increase of absorbance due to formation of P^+, and a subsequent decrease due to photooxidation of heme c-556 (Fig. 2*E*). A fit of the experimental points to a single exponential gives a rate constant of $\approx 2 \times 10^6\ s^{-1}$ ($t_{1/2} \approx 350$ ns) for heme c-556 photooxidation. In *Rps. viridis*, the highest potential heme is oxidized with a rate constant of $\approx 3 \times 10^6\ s^{-1}$ (4, 9). In this respect, our results appear to be similar to those obtained with *Rps. viridis*. In the presence of excess reduced HiPIP, on the other hand, heme c-556 photooxidation was followed by a rapid absorbance return to the baseline (Fig. 2*F*), indicating reduction of heme c-556 by HiPIP. This process, when fitted to a single exponential curve, yields a rate constant of $3.1 \times 10^5\ s^{-1}$ ($t_{1/2} = 2.2$ μs). Furthermore, the amplitude of this process decreased to zero in the presence of 100 mM NaCl (data not shown). In *Rps. viridis*, no such fast phase has ever been reported for the interaction of RC with cytochrome c_2 (22–24). In *Rf. fermentans* the fast phase does not involve electron transfer between heme c-560 (presumaby reduced in the presence of HiPIP prior to the flash) and c-556, because only in the presence of a large excess of HiPIP (64 μM) is photooxidation of c-560 detected (data not shown).

When the time course of photo-induced electron transfer was monitored at 556 nm in the absence of HiPIP, using a time resolution of 70 μs (Fig. 3*A*) and 70 ns (Fig. 3*C*), a rapid decrease of absorbance was observed, due to oxidation of heme c-556. The kinetics of this process could not be resolved

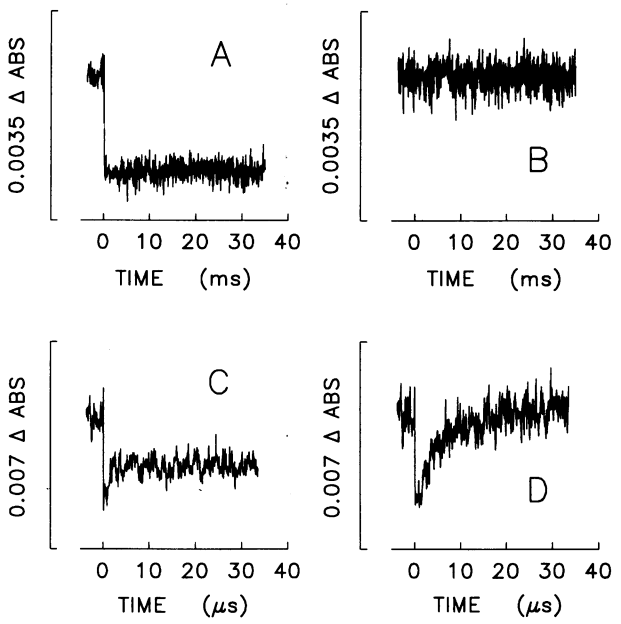

FIG. 3. Light-induced absorbance changes detected at 556 nm in the absence (*A* and *C*) or in the presence (*B* and *D*) of 10 μM HiPIP. [RC] = 3.3 μM.

because of instrumental artifacts occurring in the first 2.5 μs after the excitation flash, probably due to the proximity of excitation (610 nm) and observation (556 nm) wavelengths. No further changes in absorbance were detected up to 40 ms. In the presence of an excess of reduced HiPIP, using a time resolution of 70 μs, the signal completely disappeared (Fig. 3*B*), in agreement with the parallel observation at 425 nm (see Fig. 2*D*). However, when the reaction was monitored at 556 nm using a time resolution of 70 ns, a rapid absorbance return to the baseline, indicating reduction of heme c-556, was observed (Fig. 3*D*). The fit of the experimental points to a single exponential curve yields a rate constant of $3.3 \times 10^5\ s^{-1}$ ($t_{1/2} = 2.1$ μs), confirming the results obtained at 425 nm. Furthermore, the amplitude of the absorbance changes detected in the presence of excess HiPIP at 425 and 556 nm are in a ratio of 3.9:1, consistent with a complete reduction of heme c-556.

The value of k_{obs} for the fast phase was independent of HiPIP concentration, indicating that it is due to a first-order process, while the rate constant for the slow cytochrome reduction increased nonlinearly with HiPIP concentration, showing saturation behavior (Fig. 4*A*). Furthermore, the amplitude of the slow phase (Fig. 4*B*, solid circles) initially increased with increasing HiPIP concentration but, when HiPIP was slightly in excess of RC concentration, the signal amplitude decreased significantly. On the other hand, the amplitude of the fast phase increased monotonically with HiPIP concentration (Fig. 4*B*, open circles),

The presence of both slow and fast phases of reduction of heme c-556 in the presence of HiPIP is interpreted as being due to electron transfer occurring between HiPIP and RC free in solution or occurring within an optimally oriented electrostatic complex formed, prior to the flash, between HiPIP and RC, respectively. On the basis of the HiPIP concentration dependence of the amplitude of the fast reaction, the dissociation constant for this HiPIP–RC complex can be estimated as being ≈2.5 μM. The latter value is to be compared with the value of 0.1–10 μM for the corresponding cytochrome c_2–RC complex in *Rb. sphaeroides* (19–21, 43). The saturation behavior of the second-order plot (Fig. 4*A*), for which the reaction is second-order at low protein concentrations, but becomes first-order at high concentrations of the soluble donor, is similar to what has been observed with cytochrome c_2 in *Rps. viridis* (23, 24), *Rb.*

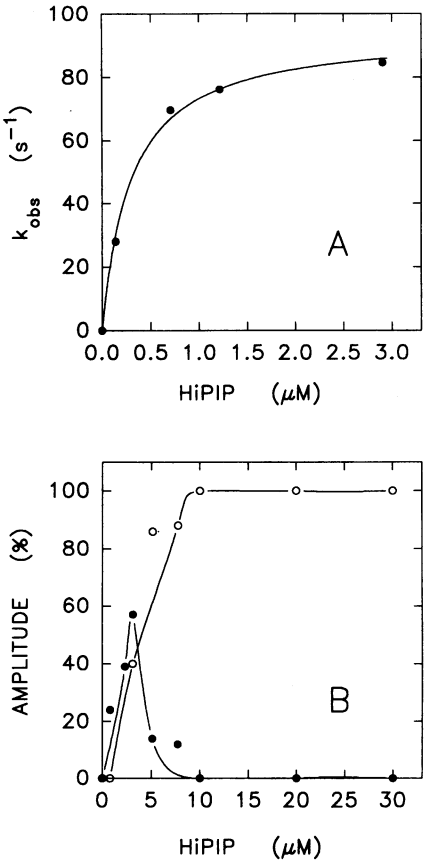

FIG. 4. (*A*) Slow phase k_{obs} for heme c-556 reduction as a function of HiPIP concentration; the solid line represents a fit of the experimental points to Eq. **1** (46). (*B*) Amplitudes of slow (solid circles) and fast phase (open circles) of heme c-556 reduction as a function of HiPIP concentration as calculated for Eq. **1** in the text. Observation wavelength was 425 nm; [RC] = 2.5 μM.

sphaeroides (14, 16, 18, 19), and *Rhodospirillum rubrum* (44) RC preparations. This behavior has been previously explained in two ways: (*i*) as due to aggregation of RC at high concentration of the soluble donor (19) or (*ii*) as due to the presence of an equilibrium involving the formation of complex between HiPIP and RC after the excitation flash, as shown in Scheme I, in which the suffixes R and O refer to the reduced or oxidized state (14, 16, 18, 19, 44, 45):

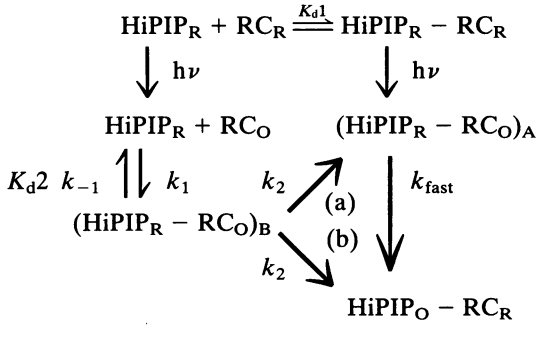

Scheme I

In this latter case, the value of k_{obs} is given by Eq. **1** (46)

$$k_{obs} = \frac{k_2[HiPIP_R]_0}{K + [HiPIP_R]_0}, \qquad [1]$$

in which $[HiPIP_R]_0$ represents the concentration of reduced HiPIP present free in solution immediately after the flash, and can be calculated assuming K_d1 = 2.5 μM. A fit of the experimental points (in Fig. 4*A*) to Eq. **1** using the calculated values of $[HiPIP_R]_0$ yields k_2 = 95 s^{-1}, and K = 0.3 μM. This limiting value of k_2, the rate constant for the slow phase, is to be compared with the analogous rate constant of 270 s^{-1} (23) or 1300 s^{-1} (24) reported for the interaction of cytochrome c_2 with RC in *Rps. viridis*. This value of k_2 is much smaller than k_{fast}, the rate constant noted above for the electron transfer in the fast phase (3.3×10^5 s^{-1}), indicating the formation of the two different types of complexes between HiPIP and RC noted above. These could be due to interaction of HiPIP and RC to give an optimal $(HiPIP_R\text{-}RC_O)_A$ or a nonoptimal $(HiPIP_R\text{-}RC_O)_B$ orientation of the proteins. The rate constant k_2 could then be interpreted as reflecting either (*a*) a slow rearrangement to obtain the optimal orientation, followed by a fast electron transfer step (the same as observed in the optimally oriented complex, with $k_{fast} = 3.3 \times 10^5$ s^{-1}), or (*b*) an electron transfer in a protein complex that does not have the optimal orientation and thus follows a different slower path. The interpretation of the parameter K in the fit of the second-order plot to Eq. **1** depends on whether the equilibrium is fast ($k_{-1} \gg k_2$) or slow ($k_{-1} \ll k_2$) (46): if the equilibrium is fast, K is the equilibrium dissociation constant K_d2 = 0.3 μM. This value is to be compared with the values of 30 μM (23) or 8.6 μM (24) for the interaction of RC and c_2 from *Rps. viridis*. If on the other hand the equilibrium is slow, one obtains $k_2/K = k_1 = 4.8 \times 10^7$ $M^{-1}\cdot s^{-1}$, the second-order rate constant for the rate-limiting step. This value is about two orders of magnitude smaller than for the reaction of *Rb. sphaeroides* cytochrome c_2 with its RC at low ionic strength (10^9 $M^{-1}\cdot s^{-1}$) (16, 18, 20), but it is similar to that of the cytochrome c_2 from *Rps. viridis* with its RC (1.3×10^8 $M^{-1}\cdot s^{-1}$) (24). As a further support to the proposed Scheme I, the amplitude dependence of the fast and the slow phase on HiPIP concentration can be qualitatively reproduced using Scheme I by assuming K_d2 = 0.3 μM and K_d1 = 2.5 μM.

The effect of ionic strength on the second-order rate constant is shown in Fig. 5. A 4-fold decrease in rate constant with increasing ionic strength is observed, consistent with electrostatic interactions between HiPIP and the RC tetraheme subunit. The effect is quantitatively similar to that obtained with cytochrome c_2 in either *Rb. sphaeroides* (47) or *Rps. viridis* (23, 24) (about 5-fold over a comparable ionic strength range). If one assumes that the ionic strength dependence of the second-order rate constant is primarily determined by ionized groups localized near the electron transfer sites, the parallel plate (Watkins) electrostatic model for

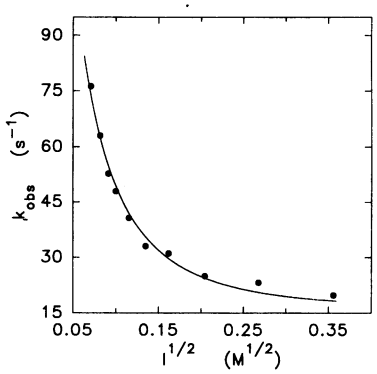

FIG. 5. Ionic strength dependence of the observed rate constant of heme c-556 reduction. [HiPIP] = 3.1 μM and [RC] = 2.5 μM. Observation wavelength was 425 nm. The solid line represents a fit of the experimental points to Eq. **2** (48), using ρ = 20 Å.

protein–protein interactions (48), can be applied. A fit of the experimental data to the following equation (48)

$$\ln k = \ln k_\infty - V_{ii}\frac{e^{-\kappa\rho}}{1+\kappa\rho}, \qquad [2]$$

in which $\kappa = 0.3295 I^{1/2}$ Å^{-1} yields values for the radius of the interaction site on the protein surfaces $\rho = 20$ Å and for the interaction energy $V_{ii} \times 0.59 = -2.1$ kcal/mol. Although the energy term is physically reasonable and consistent with a relatively moderate electrostatic interaction, it is not clear why such a large value for ρ is required to fit the data. In this model $V_{ii} = \alpha Z_1 Z_2 r_{12}/D_e\rho^2$, where $\alpha = 128.471$, Z_1 and Z_2 are the charges at the interaction site, r_{12} is the distance between the surfaces of the interacting molecules (taken as 3.5 Å, the van der Waals contact), and D_e is the effective dielectric constant at the interaction site (which is smaller than 80, the dielectric constant for water, and can be as low as 4 in the case of complete exclusion of water molecules, or 10 in the case of partial exclusion). Using $D_e = 10$ and $\rho = 20$ Å, a value of $Z_1Z_2 = -31$ can be calculated. These data thus suggest the presence of five or six specific ionic pairs between HiPIP and the tetraheme subunit, although the quantitation of the electrostatic interaction energy must be considered only approximate (48). The second-order rate constant extrapolated to infinite ionic strength $k_\infty = 5.4 \times 10^6$ M^{-1}·s^{-1} is actually a little larger than that for *Rps. viridis* cytochrome c_2 with its RC (1.2×10^6 M^{-1}·s^{-1}) (24).

In conclusion, the present study shows that HiPIP effectively reduces the photooxidized RC in *Rf. fermentans* obeying multiphasic kinetics. The reactivity of HiPIP with RC in *Rf. fermentans* is comparable to that of cytochrome c_2 with RCs from *Rb. sphaeroides* and *Rps. viridis*. Whereas cytochrome c_2 reduces the lower potential of the two high-potential hemes of the RC tetraheme subunit in *Rps. viridis*, however, *Rf. fermentans* HiPIP reduces the highest reduction potential heme, with a fast phase observed in addition to a slow phase. Whether or not HIPIP is the sole electron donor to RC or not still must be demonstrated. Our results suggest that members of the HiPIP family might function as competent electron donors to RC in other phototrophic bacteria, but this must be investigated on a case by case basis.

This work was supported in part by grants from the Fondazione Adriano Buzzati-Traverso (to A.H.), from Consiglio Nazionale delle Ricerche, Biotecnologie e Biostrumentazioni (to D.Z.), and from the National Institutes of Health, GM21277 (to M.A.C.) and DK15057 (to G.T.).

1. Feher, G. & Allen, J. P. (1989) *Nature (London)* **339,** 111–116.
2. El-Kabbani, O., Chang, C.-H., Tiede, D., Norris, J. & Schiffer, M. (1991) *Biochemistry* **30,** 5361–5369.
3. Deisenhofer, J. & Michel, H. (1989) *Science* **245,** 1463–1473.
4. Dracheva, S. M., Drachev, L. A., Konstantinov, A. A., Semenov, A. Y., Skulachev, V. P., Arutjunjan, A. M., Shuvalov, V. A. & Zaberezhnaya, S. M. (1988) *Eur. J. Biochem.* **171,** 253–264.
5. Deisenhofer, J., Epp, O., Miki, K., Huber, R. & Michel, H. (1984) *J. Mol. Biol.* **180,** 385–398.
6. Deisenhofer, J., Epp, O., Miki, K., Huber, R. & Michel, H. (1985) *Nature (London)* **318,** 618–624.
7. Nitschke, W. & Rutherford, A. W. (1989) *Biochemistry* **28,** 3161–3168.
8. Shopes, R. J., Levine, L. M. A., Holten, D. & Wraight, C. A. (1987) *Photosynth. Res.* **12,** 165–180.
9. Ortega, J. M. & Mathis, P. (1993) *Biochemistry* **32,** 1141–1151.
10. Prince, R. C., Bashford, C. L., Takamiya, K., van der Berg, W. H. & Dutton, P. L. (1978) *J. Biol. Chem.* **253,** 4137–4142.
11. Ambler, R. P., Daniel, M., Hermoso, J., Meyer, T. E., Bartsch, R. G. & Kamen, M. D. (1979) *Nature (London)* **278,** 659–660.
12. Sogabe, S., Ezoe, T., Kasai, N., Saeda, M., Uno, A., Miki, M. & Miki, K. (1994) *FEBS Lett.* **345,** 5–8.
13. Prince, R. C., Cogdell, R. J. & Crofts, A. R. (1974) *Biochim. Biophys. Acta* **347,** 1–13.
14. Dutton, P. L., Petty, K. M., Bonner, H. S. & Morse, S. D. (1975) *Biochim. Biophys. Acta* **387,** 536–556.
15. Bowyer, J. R., Tierney, G. V. & Crofts, A. R. (1979) *FEBS Lett.* **101,** 207–212.
16. Overfield, R. E., Wraight, C. A. & De Vault, D. (1979) *FEBS Lett.* **105,** 137–142.
17. Okamura, M. Y. & Feher, G. (1983) *Biophys. J.* **41,** 122a.
18. Moser, C. C. & Dutton, P. L. (1988) *Biochemistry* **27,** 2450–2461.
19. Tiede, D. M., Vashishta, A.-C. & Gunner, M. R. (1993) *Biochemistry* **32,** 4515–4531.
20. Venturoli, G., Mallardi, A. & Mathis, P. (1993) *Biochemistry* **32,** 13245–13253.
21. Lin, X., Williams, J. C., Allen, J. P. & Mathis, P. (1994) *Biochemistry* **33,** 13517–13523.
22. Shill, D. A. & Wood, P. M. (1984) *Biochim. Biophys. Acta* **764,** 1–7.
23. Knaff, D. B., Willie, A., Long, J. E., Kriauciunas, A., Durham, B. & Millett, F. (1991) *Biochemistry* **30,** 1303–1310.
24. Meyer, T. E., Bartsch, R. G., Cusanovich, M. A. & Tollin, G. (1993) *Biochemistry* **32,** 4719–4726.
25. Bartsch, R. G. (1991) *Biochim. Biophys. Acta* **1058,** 28–30.
26. Hiraishi, A., Hoshino, Y. & Satoh, T. (1991) *Arch. Microbiol.* **155,** 330–336.
27. Hochkoeppler, A., Zannoni, D. & Venturoli, G. (1995) *Biochim. Biophys. Acta* **1229,** 81–88.
28. Hochkoeppler, A., Moschettini, G. & Zannoni, D. (1995) *Biochim. Biophys. Acta* **1229,** 73–80.
29. Hochkoeppler, A., Kofod, P., Ferro, G. & Ciurli, S. (1995) *Arch. Biochem. Biophys.* **322,** 313–318.
30. Rawlings, J., Wherland, S. & Gray, H. B. (1976) *J. Am. Chem. Soc.* **98,** 2177–2180.
31. Aprahamian, G. & Feinberg, B. A. (1981) *Biochemistry* **20,** 915–919.
32. Meyer, T. E., Przysiecki, C. T., Watkins, J. A., Bhattacharyya, A., Simondsen, R. P., Cusanovich, M. A. & Tollin, G. (1983) *Proc. Natl. Acad. Sci. USA* **80,** 6740–6744.
33. Jackman, M. P., Lim, M.-C. & Sykes, A. G. (1988) *J. Chem. Soc., Dalton Trans.*, 2843–2850.
34. Bertini, I., Ciurli, S. & Luchinat, C. (1995) *Struct. Bonding* **83,** 1–53.
35. Kennel, S. J., Bartsch, R. G. & Kamen, M. D. (1972) *Biophys. J.* **12,** 882–896.
36. Evans, M. C. W., Lord, A. V. & Reeves, S. G. (1974) *Biochem. J.* **138,** 177–183.
37. Dutton, P. L. & Leigh, J. S. (1975) *Biochim. Biophys. Acta* **314,** 178–190.
38. Hochkoeppler, A., Ciurli, S., Venturoli, G. & Zannoni, D. (1995) *FEBS Lett.* **357,** 70–74.
39. Schoepp, B., Parot, P., Menin, L., Gaillard, J., Richaud, P. & Vermeglio, A. (1995) *Biochemistry* **34,** 11736–11742.
40. Tollin, G. & Hazzard, J. T. (1991) *Arch. Biochem. Biophys.* **287,** 1–7.
41. Nitschke, W. & Dracheva, S. M. (1995) *Anoxygenic Photosynthetic Bacteria*, eds. Blankenship, R. E., Madigan, M. T. & Bauer, C. E. (Kluwer, Dordrecht, The Netherlands), pp. 775–805.
42. Fukushima, A., Matsuura, K., Shimada, K. & Satoh, T. (1988) *Biochim. Biophys. Acta* **933,** 399–405.
43. Long, J. E., Durham, B., Okamura, M. & Millett, F. (1989) *Biochemistry* **28,** 6970–6974.
44. Rickle, G. K. & Cusanovich, M. A. (1979) *Arch. Biochem. Biophys.* **197,** 589–598.
45. Overfield, R. E. & Wraight, C. A. (1980) *Biochemistry* **19,** 3322–3327.
46. Strickland, S., Palmer, G. & Massey, V. (1975) *J. Biol. Chem.* **250,** 4048–4052.
47. Hall, J., Zha, X., Durham, B., O'Brien, P., Vieira, B., Davis, D., Okamura, M. & Millett, F. (1987) *Biochemistry* **26,** 4494–4500.
48. Watkins, J. A., Cusanovich, M. A., Meyer, T. E. & Tollin, G. (1994) *Protein Sci.* **3,** 2104–2114.